Energy Conversion and Management 52 (2011) 1414–1425

Contents lists available at ScienceDirect

Energy Conversion and Management

journal homepage: www.elsevier.com/locate/enconman

Performance evaluation of a once-through multi-stage flash distillation system: Impact of brine heater fouling

Hasan Baig, Mohamed A. Antar *, Syed M. Zubair

Mechanical Engineering Department, KFUPM, Saudi Arabia

ARTICLE INFO

Article history:
Received 13 April 2009
Received in revised form 30 January 2010
Accepted 3 October 2010
Available online 4 November 2010

Keywords:
Water
Desalination
Once-through
Performance
Fouling
MSF

ABSTRACT

Multi-stage flash distillation (MSF) system modeling involves a number of process variables. An estimation of all these process variables requires both analytical solutions and experimental/field analysis. However, the accurate estimate of variables related to the brine heater operation in a MSF system is very important for a reliable operation of the system. For example, steam operating conditions as well as the brine properties including fouling of the brine heater tubes have a significant effect on the heat transfer characteristics of the brine heater, which in turn influence the distillate output from the system. In this study, the effect of various design as well as operating conditions on the performance ratio (PR), brine temperature and salinity as it leaves the last flash stage are investigated in a once-through system. Increasing the number of stages from 24 to 32 has a significant effect on the PR, it ranges between 79% (for $\Delta T = 1.5$) and 327% (for $\Delta T = 2.3$) for a top-brine temperature of 106 °C. This value increase as the top-brine temperature increases. Increasing the stage-to-stage temperature difference increases the water salinity as it leaves the final stage and reduces its temperature that would imply better energy utilization within the plant. Results show that brine side heat exchanger fouling has a significant effect in decreasing the overall heat transfer coefficient, which reduces the production rate as the fouling increases with time. A sensitivity analysis to identify the key parameters, which can have a significant influence on the desalination plant performance, is carried out in an attempt to contribute a better understanding and operation of MSF desalination processes.

1. Introduction

Thermal processes hold a strong position in the water desalination market, particularly in places where they are coupled with the production of electrical power. According to Wangnick [1], about 76% (11.88×10^6 m^3/d) of all thermal MSF plants in the world (15.7×10^6 m^3/d) are installed on the Arabian Peninsula, with the United Arab Emirates having the largest installed or contracted capacity with 4.8×10^6 m^3/d, followed by Saudi Arabia with 4.0×10^6 m^3/d. Although this process is costly, it is widely used because of the attractiveness in operating dual-purpose power and water desalination plants. It is important to note that MSF plants mainly need thermal energy, which is supplied in the form of steam at low pressure compared to the steam requirement for a power plant. Steam for MSF desalination plants can be a dedicated or non-dedicated (co-generation) plant. The former provides energy exclusively for the desalination process and water is the only product out of the complex. The latter provides part of its energy to the desalination process, and the rest of the energy is used to generate electricity.

Co-generation is an economically attractive option for desalination because the cost of plant is allocated to two product streams and therefore resulting in a high utilization factor. Recently, a number of large co-generation power and desalination plants have been built in various parts of the world. For instance, combined power and water production represents the largest use of co-generation concept with over 25,000 MW of installed world electrical capacity [2]. The multi-stage flash (MSF) desalination plant utilizes excess steam available from these power-generating units mostly during the heat rejection process of a MSF plant. It is important to emphasize that dual-purpose desalination plants have several advantages over single operated plants. For example, they require less manpower, fuel consumption and financial investment [4] thus highlight their importance and application in the Arabian Gulf region.

The once-through MSF plant is an applied desalination method particularly known for its simplicity and a small number of components. The consumption of chemicals for on-line scale removal in the plant is also limited. While comparing with the brine-recycle MSF plants, the once-through MSF plants have several advantages. These are summarized by Wangnick [1] as:

- Savings of equipment (pumps, valves and other armatures) and of reduced pumping power due to the elimination of the brine-recycle loop and the heat rejection section.

* Corresponding author. Tel.: +966 38602964; fax: +966 38602949.
E-mail address: antar@kfupm.edu.sa (M.A. Antar).

0196-8904/$ - see front matter © 2010 Elsevier Ltd. All rights reserved.
doi:10.1016/j.enconman.2010.10.004

Nomenclature

Symbols

A_b	brine heater surface area (m^2)
A_c	condenser surface area for one stage (m^2)
A_s	cross sectional area of each stage, $A_s = L\ W$ (m^2)
A_t	total heat-transfer surface area (m^2)
BPE	boiling point elevation (°C)
C_p	specific heat of the seawater
C_d	weir friction coefficient
d_o	outside diameter of the tube (M)
d_i	inside diameter of the tube (M)
D_i	mass flow rate of the distillate in the *i*th stage (kg/s)
$h_{seawater}$	convective heat transfer coefficient on the water side (W/m^2 K)
$h_{steamside}$	convective heat transfer coefficient on the steam-side (W/m^2 K)
h_{fg}	latent heat (W)
h_o	convective heat transfer coefficient on the outer side of the tube (W/m^2 K)
h_i	convective heat transfer coefficient on the inner side of the tube (W/m^2 K)
H_i	height of the brine pool of the *i*th stage (m)
GH_i	gate height of the *i*th stage (m)
L	length (m)
$\dot{m}$	mass flow rate (kg/s)
N	total number of stages (–)
NEA	non-equilibrium allowance (°C)
PR	performance ratio (–)
Pr	Prandtl number (–)
R	thermal resistance (°C m^2/W)
Re	Reynolds number (–)
S_A	specific heat-transfer area (m^2/(kg/s))
T_{av}	average temperature, $T_{av} = (T_o + T_n)/n$ (°C)
T_f	feed seawater temperature (°C)
T_o	top-brine temperature (°C)
T_s	steam temperature (°C)
T_b	temperature of brine blow down (°C)
t	temperature of feed seawater in the stage's condenser (°C)
U	overall heat transfer coefficient (W/m^2 °C)
u	velocity (m/s)
V_b	brine mass flow rate per stage width (kg/m s)
V_n	vapor velocity in the last stage (m/s)
W	width (m)
x_f	intake seawater salt concentration (ppm)
x_i	salt concentration of brine stream leaving stage I, $x_i = \dot{m}_f x_f / B_i$ (ppm)
y	specific ratio of sensible heat and latent heat, $y = C_p \Delta T / h_{fg}$ (–)

Greek symbols

μ	viscosity (kg/m s)
ρ	density (kg/m^3)

Subscripts

B	brine
D	distillate
F	total flow rate (feed water)
lm	log mean
S	steam

- Savings in heat-transfer area and/or thermal energy consumption because of the lower boiling point elevation in each stage owing to lower salinity of the flashing brine.
- Reduced risk of calcium sulphate scaling due to the lower salt concentration levels, which allows higher maximum brine temperature.

The literature reveals little attention to understand the detailed modeling of its components especially the brine heater, which plays a very vital role in the analysis of MSF plants. Hamed et al. [3] carried out a thermo-economic analysis of MSF plants in Saudi Arabia. They found that of all the subsystems of the plant, particularly the flashing chamber and the brine heater contribute to the major thermodynamic losses. For example, an increase of steam temperature in the brine heater from 95 °C to 105 °C results in about 30% increase in thermodynamic losses. Helal [5] investigated the feasibility of improving the once-through MSF design using both the long- and cross-tube configurations for constructing large-capacity desalting plants in comparison to the conventional brine-recycle MSF systems. A comparison of specific heat-transfer areas (in m^2/kg s) calculated for the different plant configurations having 40 as a total number of stages. Results revealed that for the same water capacity and the same gained output ratio (GOR) is obtained from a long-tube MSF plant that shows about 40% reduction in heat-transfer area relative to the conventional cross-tube brine-recycle MSF plant design.

Nevertheless, when comparing the specific heat-transfer areas obtained from the global optimal designs of different configurations, having different numbers of stages, it is found that the use of once-through designs is not likely to save more than 1% in heat-transfer area relative to the conventional MSF configuration. These brine-recycle MSF systems use far less chemicals for makeup pretreatment. It is important to note that consumption of chemicals depends on the amount of seawater to be treated as well as the concentration ratio. Although dosing rate, in ppm, is less for the once-through system, since the seawater (intake) has the same feed concentration, the large intake flow rate calls for high rate of chemical dosing than in the recycle system. The overall result is higher overall chemical consumption in the once-through system. Therefore, it is important that the increase in operating cost due to excessive chemical consumption has to be compared against the savings in pumping and capital in civil works. Recently, ElMoudir et al. [6] pointed out the difficulties encountered while modeling especially when the plant is older. They developed Excel spreadsheets for modeling the MSF system. In addition, they pointed out the crucial part of fouling in calculating the heat-transfer areas of the plant.

El-Dessouky et al. [7] developed an algorithm for investigation steady-state behavior of the MSF desalination system. The performance equations describing the number of design and operating variables for any stage are divided into subsets describing the processes of individual components of the plant and their interdependent relationship. They demonstrated the dependence of important factors controlling the fresh water cost, which showed excellent agreement with the published data of a typical MSF plant in Kuwait. Hamed et al. [8] conducted a comparative study on energy and exergy analyses for different MSF plants. In their study, the impact of different design and operating parameters such as the top-brine temperature and number of flashing stages is highlighted. They indicated the most of the exergy losses are found in the brine heater and that increasing the number of stages increases the plant second law efficiency. Kahraman and Cengel [9] carried out a second law (Exergy) analysis for a MSF desalination plant making an exergy flow diagram indicating the areas of high exergy

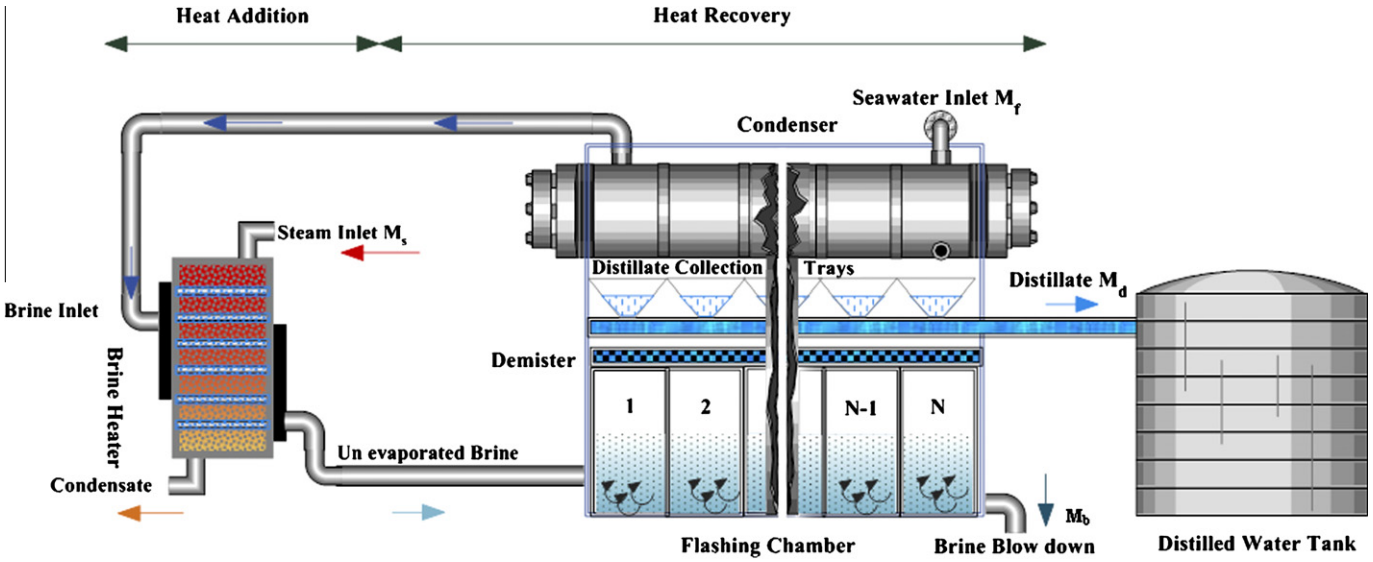

Fig. 1. A process description of a once-through multi-stage flash distillation process.

destruction, that is, flashing stages. They also reported that increasing the number of stages is an effective way to improve the plant second law efficiency.

2. Once-through multi-stage flash distillation system

A once-through MSF plant consists of two basic sections, a heat addition section and a heat recovery section as can be seen in Fig. 1. The heat recovery section consists of a condenser, the distillate collection trays and the flashing chamber. On the other hand, the heat addition section consists mainly of a brine heater. It is important to note that in the heat addition system the thermal energy of relatively low-pressure steam, exiting from the power plant is transferred to the incoming seawater; thus the sea water is heated to a temperature of around 100 °C. However, in the heat recovery section, the thermal energy from the water vapor generated during the flashing process is recovered by condensing the water vapor via the inlet sea water, which acts as a coolant.

Referring to Fig. 1, seawater at a mass flow rate of $\dot{m}_f$ enters the condenser (or heat recovery section) with salinity x_f and temperature T_{cw}. The condenser consists of n stages, as the seawater passes through each stage of the condenser, the flashing vapor heats up. Its temperature changes from T_{cw} to t_1. It should be noted that the intake seawater flows from stage n to stage 1, i.e., from the low- to high-temperature stage of the condenser. This heated seawater is then passed through the brine heater, which is most important part of the heat addition system. Here, a relatively low-pressure (around 1–2 MPa) steam is used to heat the saline water entering the brine heater. During this process, steam releases latent heat of condensation to the sea water. The condensate leaves the brine heater, which is pumped back to the steam generator of the power plant. The heated seawater leaving the heater is at the top-brine temperature, T_o, which is then directed to the flashing chambers.

The flashing chamber consists of several flashing stages whose number varies within a wide range, typically from 15 to 40. The pressure inside these flashing chambers is maintained at some what lower than the atmospheric pressure, which is reduced from stage-to-stage so that the heated seawater flashes out at a lower temperature in the successive stages. As the water flows through these chambers, the temperature decreases from T_o to T_n. The resulting vapor condenses on outside of the tube bundles in the condenser, thereby producing pure distillate water. The distillate is collected in the collection trays, which is transferred to a collection tank at a mass flow rate of $\dot{m}_d$. In order to keep the water in clean form, the flashing vapor is first passed through a demister, which avoids any liquid droplets entrained in a vapor stream otherwise the distillate vapor would be contaminated with salt. In the final flashing stage where the lowest pressure is maintained, saline water at a mass flow rate of $\dot{m}_b$ is discarded at a temperature of T_n. It should be noted that the flashing process reduces the brine temperature, while it increases the salinity from x_f to x_b in the final stage.

A careful examination of the literature indicates that some assumptions were considered by most of the investigators that idealizes the whole process such as average temperature and salinity independent properties for most of the processes occurring in the once-through system. In addition, the impact of fouling as well as stage-to-stage temperature difference was not considered by previous investigators. The objective of this paper is to consider all the above stated effects to reach to a more "realistic" performance indicators and plant characteristics. In addition, a sensitivity analysis was carried out to identify the most influential design as well as operational parameters of the MSF plant.

3. Process modeling

To carry out the mathematical modeling of the MSF plant, the following assumptions are made: (a) the temperature drop across each flashing stage as well as the temperature rise in each condenser stage is equal; (b) The effect of boiling point rise and non-equilibrium losses on the stage energy balance is considered negligible. However, their effects are included in the design of the condenser heat-transfer area.

3.1. Essential elements of the model

Fig. 1 shows that there is one input and two output streams for the plant. In this section, important equations describing mass and energy conservation are explained to model the main components involved in the MSF system. It is important to note that basic modeling of the once-through system is described elsewhere [12].

Therefore, details of the model are not repeated here, only essential elements dealing with mass and energy balances will be stated. The effect of parameters such as stage-to-stage temperature difference, fouling in the brine heater is considered in the present investigation. Furthermore, recent and updated correlations for brine properties that are described as a function of temperature and salinity are also considered.

3.2. Seawater stream

Seawater intake is usually located some distance away from the shore to ensure its clarity. The water first passes through a screen in order to filter the seaweeds and the marine life. It is then passed through a tank where it is treated with chlorine before entering the condenser of MSF plant at a mass flow rate $\dot{m}_f$. The inlet feed water $\dot{m}_f$ has a salinity of x_f. As it progresses through the entire plant, it is divided into two streams namely the distillate stream at a mass flow rate of $\dot{m}_d$ having zero salinity and the brine reject stream, $\dot{m}_b$ at a salinity of x_b. Thus, the mass balance can be written as

$$\dot{m}_f = \dot{m}_d + \dot{m}_b \tag{1}$$

In addition, the salinity balance is

$$\dot{m}_f x_f = \dot{m}_d + \dot{m}_b x_b \tag{2}$$

3.3. Flashing and the condenser stages

There are four important variables in the complete plant whose temperatures are critical for the overall plant performance. These are:

(a) Feed water inlet temperature, T_f
(b) Temperature of steam entering the brine heater, T_s
(c) Temperature of seawater leaving the brine heater, also known as the top-brine temperature, T_o
(d) Temperature of brine leaving the last stage of the flashing chamber, T_n.

In the flashing chamber, the temperature drop is considered equal in every stage, which can be calculated by,

$$\Delta T = (T_o - T_n)/n \tag{3}$$

where n is the number of flashing stages. The stage heat balance leads to:

$$\begin{aligned} &D_i C_p(T_i)T_i + \dot{m}_{B,i} C_p(T_i, x_i)T_i - D_{i+1} C_p(T_{i+1})T_{i+1} \\ &\quad - \dot{m}_{B,i+1} C_p(T_{i+1}, x_{i+1})T_{i+1} \\ &\quad = \dot{m}_f * [C_p(t_i, x_i)t_i - C_p(t_{i+1}.x_{i+1})t_{i+1}] \end{aligned} \tag{4}$$

We notice from the above equation that if we neglect the variation in specific heat with respect to temperature and salinity within the flashing chamber, this leads to simplified equal temperature rise in the sea water to the temperature drop of the brine in the flashing chamber, i.e., $\Delta T_i = \Delta t_i$. Our calculations indicate that the effect of constant C_p at a given stage is not more than ±1%, the temperature at each stage can be expressed by the relationship,

$$T_i = T_o - i\Delta T \tag{5}$$

$$t_i = T_f + [n - (i-1)]\Delta t \tag{6}$$

here 'i' represents the stage number.

3.4. Mass balance in each flashing stage

The total distillate is obtained by summing up the mass of distillate formed in each stage, D_i. Mathematically, this can be written as [11]

$$\dot{m}_d = \sum_{i=1}^{n} D_i = \dot{m}_f[1 - (1-y)^n] \tag{7}$$

The amount of brine and its salinity for a particular stage is calculated by using the correlation described by [7],

$$\dot{m}_B = \dot{m}_f - \sum_{k=1}^{i} D_k \tag{8}$$

3.5. Brine heater

Brine heaters can be of different configuration; in the present case, we consider the brine heater to be a shell-and-tube type condenser. The feed seawater $\dot{m}_f$ enters the heater tubes where its temperature increases, while the steam with a flow rate $\dot{m}_s$ condenses on outside surface of the tubes. The brine heater is considered to have an average overall heat transfer coefficient, U. The feed seawater $\dot{m}_f$ absorbs the latent heat of condensation. Its temperature increases to the maximum design value known as the top-brine temperature T_o. This value depends on the condition of steam that is available for the heater such as, the operating pressure, number of tubes in the heater, tube size, overall heat transfer coefficient as well as both mass flow rates of feed water and steam.

Considering no heat loss to the surroundings and assuming that saturated steam is entering the heater, energy balance gives,

$$\dot{m}_s h_{fg} = \dot{m}_f C_p(T_o - t_1) \tag{9}$$

where $\dot{m}_s$ is steam flow rate, h_{fg} is the latent heat of condensation at steam saturation temperature T_s and C_p is the specific heat of feed water calculated at an average of inlet and outlet temperatures of the feed water through the brine heater. The specific heat of sea water as a function of temperature and salinity is described in the appendix.

The fundamental design equation of the heater in terms of mean overall heat transfer coefficient, U_m and log mean temperature difference, ΔT_{lm} is expressed as

$$Q = U_m A_o \Delta T_{lm} \tag{10}$$

where

$$\Delta T_{lm} = \frac{\Delta T_1 - \Delta T_2}{\ln\left(\frac{\Delta T_1}{\Delta T_2}\right)} \tag{11}$$

The overall heat transfer coefficient in terms of various heat transfer resistances can be written as [13],

$$\frac{1}{U_m} = \frac{1}{h_o} + R_{fo} + A_o R_w + \left(R_{fi} + \frac{1}{h_i}\right)\frac{A_o}{A_i} \tag{12}$$

here U_m is based on the outer heat-transfer surface area, also represented in the simplified form as

$$\frac{1}{U_m} = \frac{1}{h_o} + R_t + \frac{A_o}{A_i}\frac{1}{h_i} \tag{13}$$

In the above equation, R_t is the combined thermal resistance of the tube wall and fouling.

3.6. Heat transfer coefficient on waterside

To calculate the heat transfer coefficient on the water side, typically the correlation that were developed by Dittus and Boelter [12], can be written as,

$$h_{waterside} = A(k_b/d_i)Re^B Pr^C \left(\frac{\mu_w}{\mu_b}\right)^D \quad (14)$$

where

$$Re = \frac{\rho_b u d}{\mu}, \quad Pr = \frac{\mu c_{P,b}}{k_b} \quad (15)$$

where A, B, C and D are constants. These equations do not account for the salinity of water. Other modified equations as suggested in Ref. [10] are compared in Fig. 2. For the present study, the heat transfer coefficient on the water and steam-side, respectively, are given by [10]

$$h_{seawater} = (0.656u)^{0.8}\left(\frac{d_i}{d_o}\right)\left[\frac{3293.5 + T(84.24 - 0.1714T) - X_f(8.471 + 0.1161X_f + 0.2716T)}{(d_i 100/1.7272)^{0.2}}\right] \quad (16)$$

$$h_{steam} = A\left(\frac{k^3\rho^2 g q_s}{N_{TR} d_o \Delta T_w \mu}\right)^{0.25} C_1 C_2 C_3 \quad (17)$$

The coefficients C_1, C_2 and C_3 are presented by several researchers, which have led to a range of heat transfer coefficient values as demonstrated in Fig. 3.

3.7. Overall heat transfer coefficient

The overall heat transfer coefficient computed from Eq. (11) is calculated initially by considering the condenser to be clean, i.e., with no fouling resistance. In this regard, a comparison between the U values calculated and that reported in reference [11] by several authors is presented in Fig. 4. In order to design the brine heater for the number of tubes, tube passes, tube diameter and flow velocity inside the tubes, the following procedure is adopted.

The flow rate of the heating steam, $\dot{m}_s$ is obtained from the energy balance of the brine heater, given by

$$\dot{m}_s h_{fg} = \dot{m}_f C_p (T_o - t_i) \quad (18)$$

3.8. Heat-transfer areas

The brine heater and condenser surface areas may be calculated from Eq. (9). In this regard, the log mean temperature difference across the brine heater can be written as,

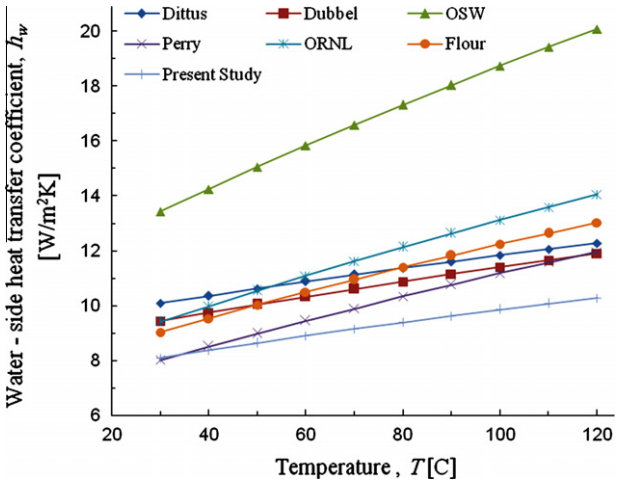

Fig. 2. Comparison of heat transfer coefficient on the waterside of the brine heater.

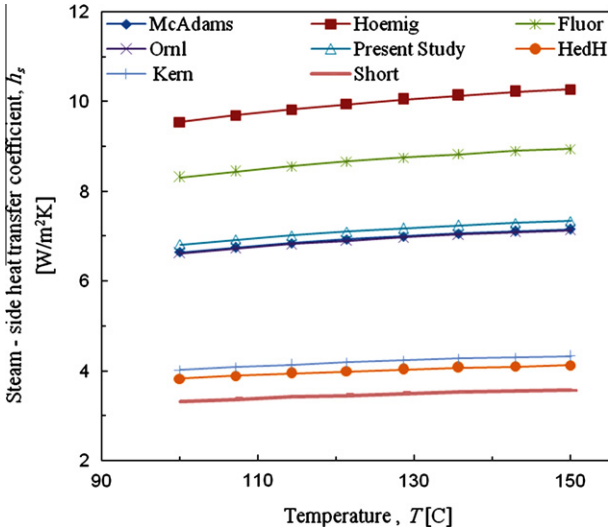

Fig. 3. Comparison of heat transfer coefficient on the steam-side of the brine heater.

$$(LMTD)_b = ((T_s - T_o) - (T_s - t_1))/\ln((T_s - T_o)/(T_s - t_i)) \quad (19)$$

The brine heater heat-transfer area required in terms of the number of tubes and their length L are expressed as,

$$A_b = N_t \pi d_o L_e \quad (20)$$

where the number of tubes are

$$N_t = \frac{\dot{m}_f}{\left(u\rho\frac{\pi}{4}d_i^2\right)} \quad (21)$$

The heat-transfer area for the condenser in each stage is assumed equal. Therefore, the calculated heat-transfer area for the first stage is used to obtain the total heat-transfer area in the plant. The condenser heat-transfer area in the first stage can be obtained from

$$A_c = \frac{\dot{m}_f C_p (t_1 - t_2)}{U_c (LMTD)_c} \quad (22)$$

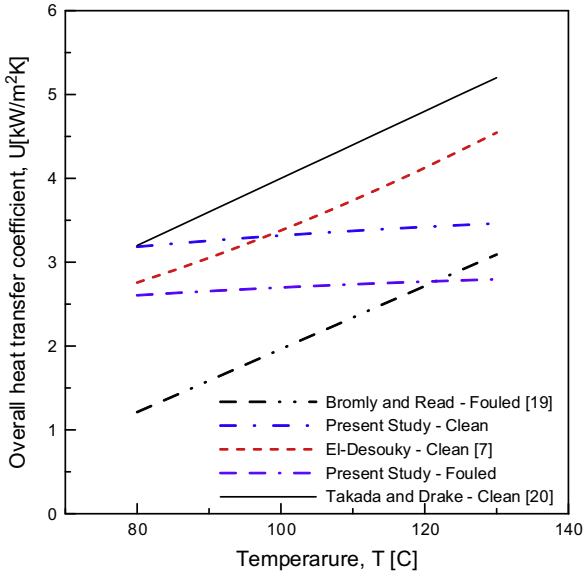

Fig. 4. Comparison of overall heat transfer coefficient of the brine heater for clean conditions. (See above-mentioned references for further information.)

where U_c is calculated from the empirical correlation described in [11]. The condensing vapor temperature, T_{v1} is obtained using the standard relationship [7]

$$T_{v1} = T_1 - \mathrm{BPE}_1 - \mathrm{NEA}_1 - \Delta T_{d1} \quad (23)$$

The expressions used for calculating the boiling point elevation (BPE), non-equilibrium allowance (NEA), and the temperature drop in the demister (ΔT_{d1}) are given in Appendix A.

$$(LMTD)_c = ((T_{v1} - t_1) - (T_{v1} - t_2))/\ln((T_{v1} - t_1)/(T_{v1} - t_2)) \quad (24)$$

The total heat-transfer area A_t of the plant is obtained by summing the heat-transfer area for all the condensers and the brine heater.

3.9. Flashing stage dimensions

The calculation of the flashing stage dimensions (gate height, GH and brine pool height, H and width W) can be expressed as [7]

$$GH_i = \frac{\left(\dot{m}_f - \sum_{j=1}^{i-1} D_j\right)(2P_{b,i} - \Delta P_i)^{(-0.5)}}{C_d W} \quad (25)$$

where

$$H_i = 0.2 + GH_i \quad (26)$$

and the width of the chamber is given by,

$$W = \frac{\dot{m}_f}{V_b} \quad (27)$$

here V_b is the brine mass velocity per unit chamber width. The length of the last stage is calculated by

$$L = D_n/(\rho_{vn} V_{vn} W) \quad (28)$$

3.10. Performance parameters

The thermal performance of the desalination plants is generally expressed in terms of performance ratio (PR) defined as the amount of distillate produced per unit of steam consumption. In addition, specific heat-transfer area is also used to determine the heat-transfer area required per unit mass of the distillate produced, S_A. These are expressed as,

$$\mathrm{PR} = \frac{\dot{m}_d}{\dot{m}_s}, \quad S_A = \frac{A_t}{\dot{m}_d} \quad (29)$$

4. Results and discussion

In this study, a mathematical model that is described above is used to investigate the important design parameters of once-through MSF system, which can influence the system performance. These parameters are:

(a) Top-brine temperature, T_o
(b) Number of flashing stages, N
(c) Fouling resistance, R_f
(d) Seawater salinity throughout the process
(e) Pressure variation inside the flashing stages
(f) Temperature drop in each stage, ΔT
(g) Mass flow rate of the steam ($\dot{m}_s$) and sea water at different stages
(h) Overall heat transfer coefficient, U
(i) Heat-transfer area, A_T
(j) Performance ratio, PR

The possibilities of improving the operation of brine heater design are also investigated. In order to carry out a comparison, a reference MSF plant is considered [22]. The possible variations in its design parameters are also investigated. The input data used in the present study is as shown in Table 1.

Table 1
Data of the reference plant [12].

Main parameter	Value (range)
Top-brine temperature, T_o	106 °C
Steam temperature, T_s	116 °C
Distillate output, $\dot{m}_d$	378.8 kg/s
Number of flashing stages	24
Salinity of the seawater at inlet	42,000 ppm
Vapor velocity in the last stage	6 m/s
Velocity of the seawater through the brine heater tube	2 m/s

4.1. Solution procedure

The salient features of the computer program that is used to simulate the performance of a once-through MSF plant can be summarized as under:

(a) Design and boundary parameters such as number of stages, top-brine temperature, temperature and salinity of seawater, and desired distillate output are input parameters to the program.
(b) Thermodynamic properties such as enthalpy (h), saturation pressure (P_{sat}) of seawater feed, steam and its condensate, seawater properties are calculated at the known input values by using appropriate correlations as explained in Appendix A.
(c) Uniform stage-to-stage temperature difference (ΔT_n) is assumed in the simulation program and is calculated by dividing flash range by total number of stages. The initial value of makeup and recycle flows is assumed. If not, the temperature of the brine leaving the plant is used to calculate temperature drop in each stage.
(d) By maintaining appropriate saturation pressure in the flashing stages, it is assumed that flashing brine in all stages is homogeneous and at saturation temperature. Flashing brine temperature (TB) of each stage is computed using the assumed equal temperature difference, while stage vapor temperatures (T_v) are calculated by determining boiling point elevation (BPE) of brine in each stage.
(e) All thermodynamic properties of the flashing brine, vapor and distillate are calculated at known fluid temperatures determined in step (d). Stage-to-stage mass and energy balances are then performed to determine the amount of vapor generated in each stage as well as salinity and flow rate of flashing brine.
(f) Mass of water, energy and flashing brine salinity balances, vapor and product distillate in every stage of an MSF unit is calculated with the known properties of step (e).
(g) Total distillate production is calculated by adding distillates of all stages. The new value of the distillate produced is then compared with the targeted distillate production.
(h) Steps (e) to (g) are repeated until the solution converges to <0.0001. The convergence achieved within a very short time (less than a second), gives complete properties and process information of flashing brine, vapor and product water.
(i) The performance results that are obtained by carrying out the above procedure are compared with the data reported in Ref. [22] as shown in Table 2.

Table 2
Comparison with the operating parameters of the reference MSF plant.

Parameter	Reference	Calculated	Parameter	Reference	Calculated
$\dot{m}_f$	3384 kg/s	3521 kg/s	PR	3.96	3.968
x_b	47292.6 ppm	47063 ppm	N_t	–	3573
$\dot{m}_s$	95.49 kg/s	95.47 kg/s	L_b	–	18.54 m
U_b	2000 W/m^2 K	2068 W/m^2 K	GH	0.078 m	0.0783 m
A_b	6481.68 m^2	6241 m^2	H	0.278 m	0.2783 m
A_t	44377.7 m^2	43935 m^2	L	2.486 m	2.58 m
C_p	4180 J/kg °C	4001–4242[a] J/kg-K,	W	18.8 m	19.56 m

[a] Function of temperature.

Table 3
Comparison between results of the present analysis with previously reported work of Helal [5].

Variable	Helal et al. [5]	Present work
PR	10	10.25
Heat transfer coefficient in the brine heater, U_b	3070 W/m^2 K	3124 W/m^2 K
Surface area of the brine heater, A_b	5681 m^2	6061 m^2
Mass flow rate of steam, m_s	105.23 kg/s	103.7 kg/s
Number of tubes in the brine heater, N_T	7546	7379
m_f	7207 kg/s	7974 kg/s

4.2. Model validation

Results of the present analysis were compared with El-desouky and Ettouney [22] in Table 2, where the results are found to be in close agreement within 4% of the reported values. Results were also compared with the analysis of Hilal [27] in Table 3. The comparison indicated very close performance parameters with a maximum percentage difference of 6%.

The sensitivity of the MSF plant is also examined as a function of the top-brine temperature and the number of flashing stages. The analysis that is presented in the following section includes effects of the system parameters on thermal performance ratio, total specific heat-transfer area, salinity of blow down brine, specific flow rates of feed, steam and blow down brine. The analysis is performed for the top-brine temperature over a range of 105–120 °C, the total number of stages varied from 16 to 35. In order to cover this range, steam temperature is increased to 130 °C.

Fig. 5 shows the effect of changing the stage-to-stage temperature drop ΔT and the number of stages on the performance ratio for top-brine temperatures of 106 °C and 110 °C. We notice that increasing the stage-to-stage temperature difference or the number of stages results in an increase in the performance ratio, PR. Keeping Δt and T_o constant, an increase in the number of stages results in lower exit temperature T_n. This means better utilization of the energy carried by steam to produce the fresh water. This trend can easily be verified mathematically by considering Eq. (7). The same result is obtained by increasing ΔT and keeping the number of stages as well as T_o fixed, since it results in decreasing T_n and hence more fresh water can be obtained. The figure also shows that PR decreases as we increase the top-brine temperature if we keep the number of stages (N), ΔT and distillate flow rate (m_d) unchanged. This is due to the decrease in the steam latent heat of condensation h_{fg} as the temperature increases resulting in higher steam flow rate and lower PR (PR = m_d/m_s), but this option is generally not recommended for actual plants.

The decrease in T_n for this case is shown in Fig. 6a for different number of stages and various values of Δt. Fig. 6a also shows the change in the brine salinity as it leaves the last stage. Increasing ΔT or increasing the number of stages means more evaporation and hence more fresh water production from the brine. Therefore, higher salt concentration is found in the brine leaving the last desalination stage (n). The same trend is also shown in Fig. 6b for T_o = 110 °C and Figs. 7a and 7b for T_o = 115 °C. However, as expected, we get different values of PR, as well as T_n and x_n result due to the change in the top-brine temperature, T_o.

Fig. 8 shows the increase in PR with top-brine temperature T_o for a fixed number of stages (N = 28), having exit brine temperature (T_n = 40 °C) and for a specified distillate flow rate (m_d). This increase is attributed to the decrease in the steam mass flow rate, higher surface area in brine heater as well as stages. It is also evident from the figure that the specific area increases with T_o, which means higher surface area for both the brine heaters and the flashing stages. To summarize, one can say that increasing the number of stages, stage-to-stage temperature difference increase the performance ratio. It is important to emphasize that increasing the number of stages is important for a once-through system, since it is an effective way to make use of the energy carried by the steam in the absence of brine recycling process.

4.3. Effect of fouling

The deposition of undesirable substances on the tube surface; result in heat exchanger performance degradation. This process is defined as fouling of heat exchangers. It plays a significant role in the design of a heat exchanger as a source of economic and operating losses. Accordingly, fouling effects are considered in the brine heater design. The effect of fouling resistance on the inside surface of the tube is shown in Figs. 9 and 10.

We notice that increasing fouling resistance decreases the overall heat transfer coefficient, considerably. In Fig. 9, fouling resistance R_{fi} is varied from 0 to 0.001 [m^2 K/W]. The overall heat transfer coefficient, U of the brine heater falls down from 2.5 to 6 kW/m^2 K; that is, about 400% decrease in the U value. However, it is independent of the flashing stages. It is important to note that fouling increases with the increase in operating temperatures of the brine heater because of the inverse solubility characteristics of the salts in the intake sea water.

The impact of the fouling resistance on the brine heater heat-transfer area is studied in Fig 10. It shows that the brine

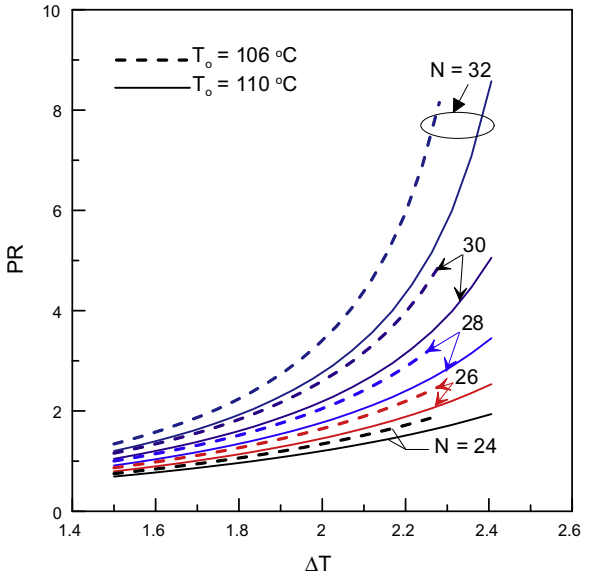

Fig. 5. Effect of ΔT and number of stages on the performance ratio, T_o = 106 °C.

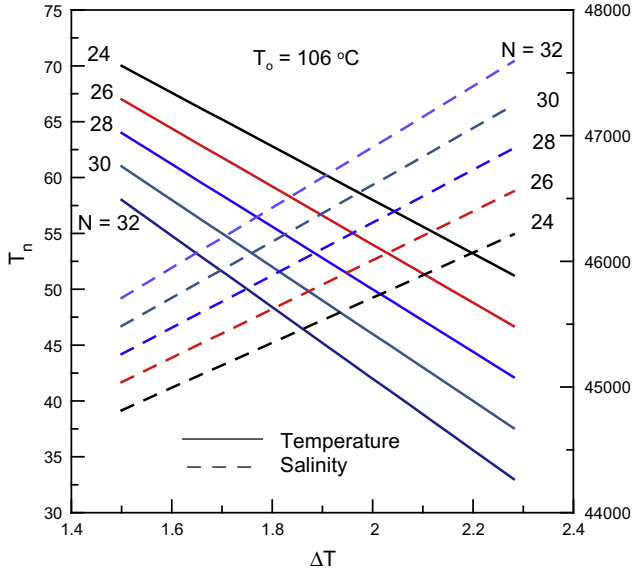

Fig. 6a. Effect of ΔT and number of stages on T_n and X_n, T_o = 106 °C.

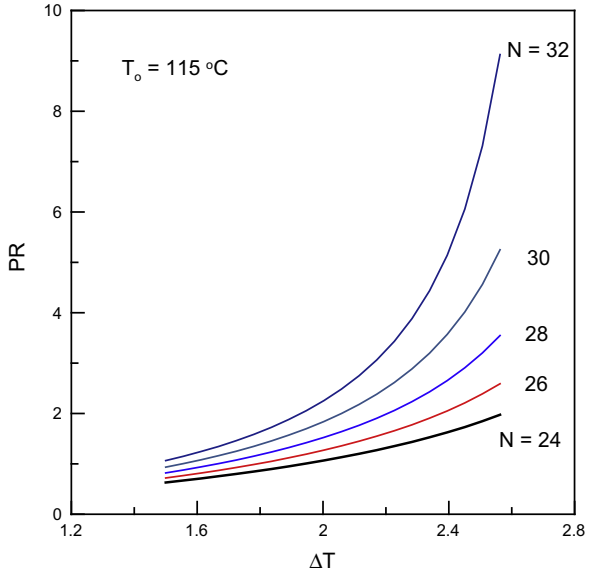

Fig. 7a. Effect of ΔT and number of stages on the performance ratio, T_o = 115 °C.

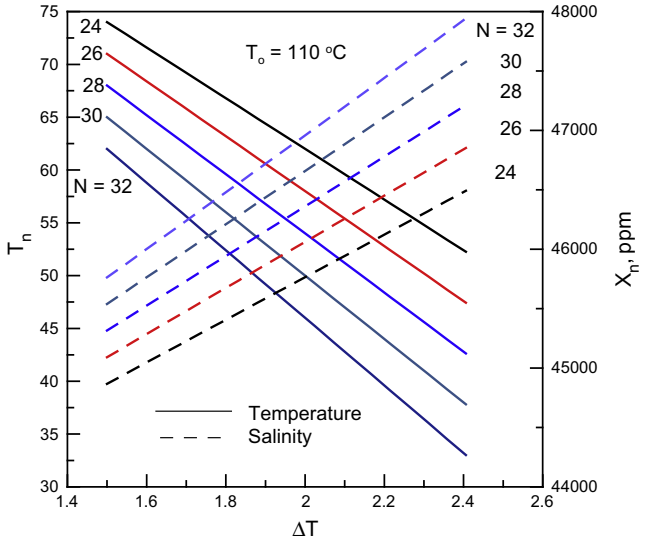

Fig. 6b. Effect of ΔT and number of stages on T_n and X_n, T_o = 110 °C.

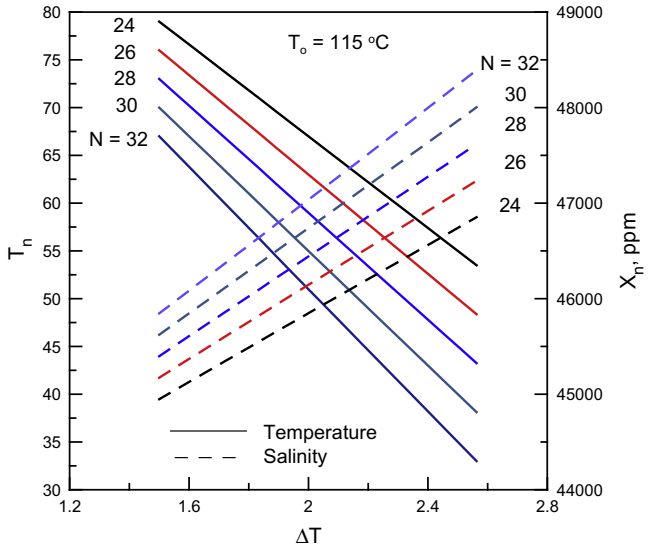

Fig. 7b. Effect of ΔT and number of stages on T_n and X_n, T_o = 115 °C.

heater surface area increases with increasing fouling resistance for a given top-brine temperature. As anticipated, the required heater surface area A_b increases with the top-brine temperature because of the less availability of latent heat of evaporation at high steam saturation temperatures. This fact implies that the increase in fouling resistance with respect to time will result in performance degradation, which should be compensated by adding additional heat-transfer area to meet the desired distillate production rate.

4.4. Sensitivity analysis

The relative importance assessment of input parameters on the performance ratio PR is obtained through estimate of the sensitivity coefficients that are described in the Appendix. Sensitivity coefficients in the present problem were evaluated for two different cases. In the first case, stage-to-stage drop is calculated from the exit and top-brine temperature, while in the second case, exit temperature from the flashing chamber is calculated by keeping fixed stage temperature drop. In this regard, Engineering Equation Solver [14] is used to compute the sensitivity coefficients and uncertainty propagation. Sensitivity coefficients in the present problem are evaluated for the eight input variables, which are shown in the tables.

Tables 4 and 5 show computed results for nominal values of the input parameters shown in Table 1. An uncertainty range of ±1 °C for temperatures, ±10% for salinity of the seawater and ±1% for seawater velocity through the brine heater tubes are considered. It is seen that the overall uncertainty in the measured Performance Ratio PR would then be of the order of 10%. It is also shown in Table 4 that the major contributor to this uncertainty is the temperature of the seawater leaving the flashing chamber in the final stage followed by the temperature of seawater entering the desalination plant. The last column (percentage uncertainty) indicates the relative contribution of each parameter towards the overall uncertainty in PR.

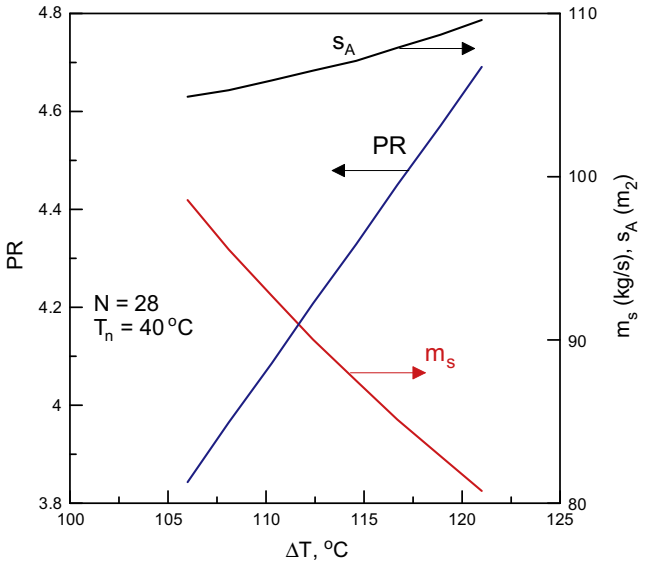

Fig. 8. The effect of T_o and ΔT on the performance ratio.

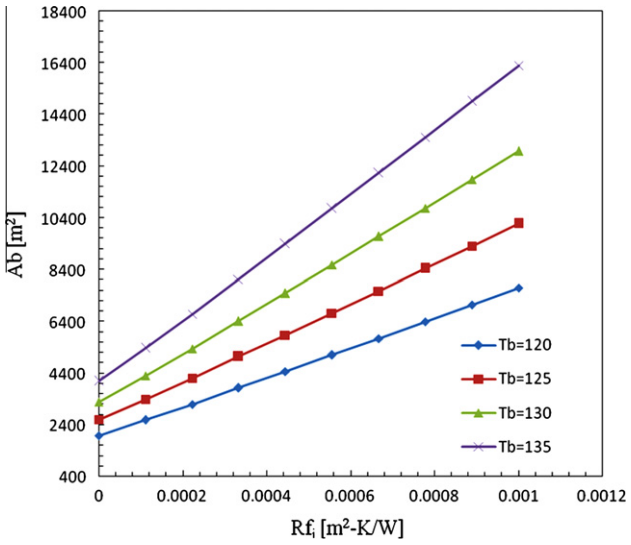

Fig. 10. Variation of the heat-transfer area of the brine heater with changing fouling resistance at different top-brine temperatures.

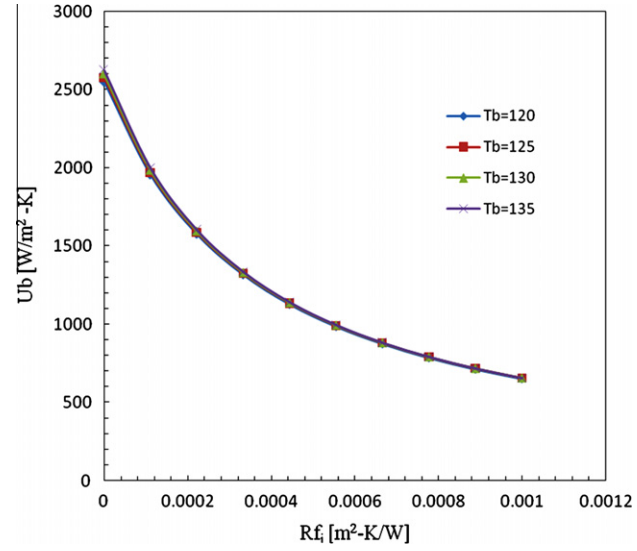

Fig. 9. Variation of the overall heat transfer coefficient as an effect of internal fouling of the tube.

In a similar manner, the uncertainty analysis of the input parameters on the calculated overall heat transfer coefficient was carried out. Results are summarized in Table 6. The table indicates that the overall uncertainty in the overall heat transfer coefficient of the brine heater would then be of the order of ±1%.

5. Concluding remarks

Thermal processes still hold a dominant share in the field of seawater desalination, especially if it is possible to couple the plant with a steam power plant or any form of waste heat recovery, or if the local conditions are difficult and there is a need for the potable water. In addition, there is considerable room for the further development of MSF plants (materials, thinner exchanger tubes, etc.) and extensive possibilities for improvement in the plant design. This study showed that the increase in top-brine temperature, number of stages, stage-to-stage temperature difference, temperature of brine leaving the last flash stage and water salinity have a significant effect on the production rate in a once-through system. Moreover, increasing the number of stages is important for a once-through system in order to make use of the energy carried by the steam in the absence of brine recycling process The effect of brine side heat exchangers fouling is significant in decreasing the overall heat transfer coefficient, which reduces the production rate. Analysis also indicated that both the temperature of the seawater leaving the flashing chamber in the final stage and the temperature of seawater entering the desalination plant have an influential effect on the performance ratio. A change in ±1 °C in either one results in a change in the PR of 58.2% and 40%, respectively.

Increasing the fouling resistance from 0 to 0.001 m^2 K/W resulted in a 400% decrease in the overall heat transfer coefficient. In addition, accounting for fouling in the design phase of the heat exchangers has a pronounced effect in increasing the required surface area. A sensitivity analysis indicates that the most influential parameters that affect the production rate are: (a) brine outlet and inlet temperatures, (b) number of stages, (c) top-brine temperature, and (d) the fouling resistance.

Table 4
Relative contribution of the input parameters towards the overall sensitivity of the Performance ratio for fixed exit temperature of seawater PR = 3.968 ± 0.419.

No.	Variable x_i	Range of variability	$\frac{d(PR)}{dx_i}$	% of Uncertainty
1	m_d	±1%	0	0
2	T_c	±1 °C	0.2645	39.86
3	T_o	±1 °C	0.0588	1.96
4	T_n	±1 °C	−0.3195	58.16
5	T_s	±1 °C	−0.004947	0.01
6	x_f	±1%	3.02E−07	0

Table 5
Relative contribution of the input parameters towards the overall sensitivity of the Performance ratio for fixed stage temperature drop PR = 3.968 ± 0.9536.

No	Variable x_i	Range of variability	$\frac{d(PR)}{dx_i}$	% of Uncertainty
1	m_d	±1%	0	0
2	T_c	±1 °C	0.2645	7.69
3	T_o	±1 °C	−0.2607	7.47
4	N	±1	0.8783	84.83
5	T_s	±1 °C	−0.004947	0
6	x_f	±1%	3.02E−07	0

Table 6
Relative contribution of the input parameters towards the overall sensitivity of the brine heater overall heat transfer coefficient U_b = 2068 ± 19.72.

No.	Variable x_i	Range of variability	$\frac{d(U_b)}{dx_i}$	% of Uncertainty
1	K_{steam}	±1%	692.8	5.52
2	μ_{steam}	±1%	−641455	2.45
3	R_{fi}	±1%	−4.751E+06	18.81
4	R_{fo}	±1	−3.959E+06	0.03
5	ρ_{steam}	±1	−0.3264	2.45
6	T_c	±1 °C	5.681	8.3
7	T_s	±1 °C	−9.016	20.91
8	T_n	±1 °C	−5.681	8.3
9	T_o	±1 °C	11.36	33.21

Acknowledgement

The support provided by KFUPM to carry out this investigation under project # SB080013 is gratefully acknowledged.

Appendix A

The calculation of the seawater properties was carried out based on the temperature, salinity and pressure according to UNESCO specifications, implemented by Millero et al. [16], while the calculation of thermodynamic losses is carried out based on the procedure recommended by El-Dessouky et al. [7]. These properties and procedures along with other important definitions introduced in the paper are summarized in this appendix. In the present study, a library has been developed by using these equations in the EES software [14].

A.1. Specific heat of salt water

Specific heat of seawater C_p (J/kg K) is a function of salinity S, temperature T and the pressure P. For seawater, the specific heat increases with the temperature and decreases with salinity and pressure. The subroutine developed to calculate the density of seawater is based on the following equations that are presented in Ref. [17]

$$C_p = C_{pst0} + \mathrm{del\_}C_{p0t0} + \mathrm{del\_}C_{pstp} \tag{A.1}$$

where

$$C_{pst0} = (((((c_4 * T_{68}) + c_3) * T_{68} + c_2) * T_{68} + c_1) * T_{68}) + c_0 + (a_0 + a_1 * T_{68} + a_2 * T_{68}^2) * S + (b_0 + b_1 * T_{68} + b_2 * T_{68}^2) * S * \mathrm{sqrt}(S) \tag{A.2}$$

$$\mathrm{del\_}C_{p0t0} = ((((cc_3 * T_{68} + cc_2) * T_{68} + cc_1) * T_{68} + cc_0) * P) + ((((((bb_4 * T_{68} + bb_3) * T_{68} + bb_2) * T_{68} + bb_1) * T_{68} + bb_0)) * P) + ((((((aa_4 * T_{68} + aa_3) * T_{68} + aa_2) * T_{68} + aa_1) * T_{68} + aa_0)) * P) \tag{A.3}$$

$$\mathrm{del\_}C_{pstp} = (((((d_4 * T_{68} + d_3) * T_{68} + d_2) * T_{68} + d_1) * T_{68} + d_0) * S + ((e_2 * T_{68} + e_1) * T_{68} + e_0) * S3\_2) * P - (((((f_3 * T_{68} + f_2) * T_{68} + f_1) * T_{68} + f_0) * S + g_0 * S3\_2) * P^2) + ((((h_2 * T_{68} + h_1) * T_{68} + h_0) * S + j_1 * T_{68} * S3\_2) * P^3) \tag{A.4}$$

and

$$S = x/1000$$

$$S3\_2 = S * \sqrt{S}$$

$$T_{68} = T * 1.00024$$

The various constants that are used in the above equation are given in Table A1.

A.2. Density of seawater

The density of seawater ρ (in kg/m^3 is a function of salinity S, temperature T and the pressure P. For seawater, the density variation is different as compared to the pure water. The following model suggested in Refs. [15,16] has been used to develop the subroutine for the seawater density calculation. The various constants used in this formulation are summarized in Table A2.

$$\rho = sw_{dens0}/(1 - P/sw_{seck}) \tag{A.5}$$

where

$$sw_{dens0} = sw_{smow} + (b_0 + (b_1 + (b_2 + (b_3 + b_4 * T_{68}) * T_{68}) * T_{68}) * T_{68}) * S + (c_0 + (c_1 + c_2 * T_{68}) * T_{68}) * S * \mathrm{sqrt}(S) + d_0 * S^2 \tag{A.6}$$

$$sw_{seck} = K_o + (A + B * P) * P \tag{A.7}$$

and

$$sw_{smow} = a_0 + (a_1 + (a_2 + (a_3 + (a_4 + a_5 * T_{68}) * T_{68}) * T_{68}) * T_{68}) * T_{68} \tag{A.8}$$

$$A = A_W + (i_0 + (i_1 + i_2 * T_{68}) * T_{68} + j_0 * SR) * S \tag{A.9}$$

$$B = B_W + (m_0 + (m_1 + m_2 * T_{68}) * T_{68}) * S \tag{A.10}$$

$$K_o = K_W + (f_0 + (f_1 + (f_2 + f_3 * T_{68}) * T_{68}) * T_{68} + (g_0 + (g_1 + g_2 * T_{68}) * T_{68}) * SR) * S \tag{A.11}$$

$$A_W = h_0 + (h_1 + (h_2 + h_3 * T_{68}) * T_{68}) * T_{68} \tag{A.12}$$

$$B_W = k_0 + (k_1 + k_2 * T_{68}) * T_{68} \tag{A.13}$$

$$K_W = e_0 + (e_1 + (e_2 + (e_3 + e_4 * T_{68}) * T_{68}) * T_{68}) * T_{68} \tag{A.14}$$

$$SR = \sqrt{(S)} \tag{A.15}$$

A.3. Thermal conductivity of seawater

The thermal conductivity of seawater as a function of temperature is defined as [11]

$$k = (10^{d_1})/1000 \tag{A.16}$$

where

$$d_1 = \log_{10}(240 + a_1 * S) + 0.434 * (2.3 - ((343.5 + b_1 * S)/(T + 273))) * (1 - ((T + 273)/(647.3 + c_1 * S)))^{1/3} \tag{A.17}$$

$$a - 1 = 0.0002, \quad b_1 = 0.037 \text{ and } c_1 = 0.03 \tag{A.18}$$

A.4. Viscosity of seawater

The correlation for dynamic viscosity of seawater (μ) is given in kg/m s, where T in °C, and S in gm/kg. This can be expressed as [11]

$$\mu = \mu_w * \mu_R * 0.001 \tag{A.19}$$

Table A1
Specific heat constants.

$a_0 = -7.64357$	$b_0 = 0.1770383$	$c_0 = 4217.4$	$d_0 = 4.9247E{-}3$	$f_0 = -2.9558E{-}6$
$a_1 = 0.1072763$	$b_1 = -4.07718E{-}3$	$c_1 = -3.720283$	$d_1 = -1.28315E{-}4$	$f_1 = 1.17054E{-}7$
$a_2 = -1.38385E{-}3$	$b_2 = 5.148E{-}5$	$c_2 = 0.1412855$	$d_2 = 9.802E{-}7$	$f_2 = -2.3905E{-}9$
$aa_0 = -4.9592E{-}1$	$bb_0 = 2.4931E{-}4$	$c_3 = -2.654387E{-}3$	$d_3 = 2.5941E{-}8$	$f_3 = 1.8448E{-}11$
$aa_1 = 1.45747E{-}2$	$bb_1 = -1.08645E{-}5$	$cc_0 = -5.422E{-}8$	$d_4 = -2.9179E{-}10$	$g_0 = 9.971E{-}8$
$aa_2 = -3.13885E{-}4$	$bb_2 = 2.87533E{-}7$	$cc_1 = 2.6380E{-}9$	$e_0 = -1.2331E{-}4$	$h_0 = 5.540E{-}10$
$aa_3 = 2.0357E{-}6$	$bb_3 = -4.0027E{-}9$	$cc_2 = -6.5637E{-}11$	$e_1 = -1.517E{-}6$	$h_1 = -1.7682E{-}11$
$aa_4 = 1.7168E{-}8$	$bb_4 = 2.2956E{-}11$	$cc_3 = 6.136E{-}13$	$e_2 = 3.122E{-}8$	$h_2 = 3.513E{-}13$
				$j_1 = -1.4300E{-}12$

Table A2
Density constants.

$a_0 = 999.842594$	$b_0 = 8.24493E{-}1$	$c_0 = -5.72466E{-}3$	$e_0 = 19652.21$	$h_0 = +3.239908$
$a_1 = 6.793952E{-}2$	$b_1 = -4.0899E{-}3$	$c_1 = +1.0227E{-}4$	$e_1 = 148.4206$	$h_1 = +1.43713E{-}3$
$a_2 = -9.095290E{-}3$	$b_2 = 7.6438E{-}5$	$c_2 = -1.6546E{-}6$	$e_2 = -2.327105$	$h_2 = +1.16092E{-}4$
$a_3 = 1.001685E{-}4$	$b_3 = -8.2467E{-}7$	$d_0 = 4.8314E{-}4$	$e_3 = 1.360477E{-}2$	$h_3 = -5.77905E{-}7$
$a_4 = -1.120083E{-}6$	$b_4 = 5.3875E{-}9$	$k_2 = 5.2787E{-}8$	$e_4 = -5.155288E{-}5$	$i_0 = 2.2838E{-}3$
$a_5 = 6.536332E{-}9$		$k_1 = -6.12293E{-}6$	$f_0 = 54.6746$	$i_1 = -1.0981E{-}5$
		$k_0 = 8.50935E{-}5$	$f_1 = -0.603459$	$i_2 = -1.6078E{-}6$
$m_0 = -9.9348E{-}7$			$f_2 = 1.09987E{-}2$	$j_0 = 1.91075E{-}4$
$g_0 = 7.944E{-}2$			$f_3 = -6.1670E{-}5$	

where

$$\mu_w = \exp(\mu_1) \tag{A.20}$$

$$\mu_1 = -3.79418 + 604.129/(139.18 + T) \tag{A.21}$$

$$\mu_R = 1 + a_2 * S + b_2 * S^2 \tag{A.22}$$

and

$$a_2 = (1.474/1000) + (1.5 * T/100000) - ((3.927 * T^2)/10^8) \tag{A.23}$$

$$b_2 = (1.0734/10^5) - ((8.5 * T)/10^8) + ((2.23 * T^2)/10^{10}) \tag{A.24}$$

The above correlation is valid over the following ranges $0 < S < 130$ gm/kg and $10 < T < 180$ °C.

A.5. Non-equilibrium allowance (NEA)

NEA represents the difference between the real temperature of the brine exiting the stage and the temperature corresponding to thermodynamic equilibrium with the prevailing pressure in the flashing vacuum. The correlations for the non-equilibrium allowance are described by Lior [18] as a function of the brine temperature, gate height, the brine flow rate per unit length of the chamber width, and the stage temperature drop

$$\mathrm{NEA} = (0.9784) * T_i * (15.7378) * H * (1.3777)^{V_{b\times 10^{-6}}} \tag{A.25}$$

where T_i is the stage temperature in °C, H is the height of the brine pool in m, and V_b is the brine flow rate per unit length of the chamber width in kg/(m s).

A.6. Boiling point elevation

The boiling point elevation represents the rise in the boiling point due to presence of salinity inside the brine solution. The correlation for the boiling point elevation of seawater can be expressed as [12]

$$\mathrm{BPE} = Ax + Bx^2 + Cx^3 \tag{A.26}$$

$$A = (8.325 * 10^{-2} + 1.883 * 10^{-4} * T + 4.02 * 10^{-6} * T^2) \tag{A.27}$$

$$B = (-7.625 * 10^{-4} + 9.02 * 10^{-5} * T - 5.2 * 10^{-7} * T^2) \tag{A.28}$$

$$C = (1.522 * 10^{-4} - 3 * 10^{-6} * T - 3 * 10^{-8} * T^2) \tag{A.29}$$

where T is the temperature in °C and X is the salt weight percentage. The above equation is valid over the range: $1 < x < 16\%$, $10 < T < 180$ °C.

A.7. On uncertainty analysis

Any independent variable can be represented as

$$X = \overline{X} \pm U_X \tag{A.30}$$

where X denotes its nominal value and U_X its uncertainty about the nominal value. The $\pm U_X$ interval is defined as the band within which the true value of the variable X can be expected to lie with a certain level of confidence (typically 95%). On the other hand, if a function $Y(X)$ represents an output parameter, then the uncertainty in Y due to an uncertainty in X is expressed in a differential form as [21]

$$U_Y = \frac{dY}{dX} U_X \tag{A.31}$$

For a multi-variable function $Y = Y(X_1, X_2, X_3, \ldots, X_N)$, the uncertainty in Y due to uncertainties in the independent variables is given by the root sum square product of the individual uncertainties computed to first order accuracy as

$$U_Y = \left[\sum_{i=1}^{N} \left(\frac{\partial y}{\partial x} U_{X_i}\right)^2\right]^{1/2} \tag{A.32}$$

Physically, each partial derivative in the above equation represents the sensitivity of the parameter Y to small changes in the independent variable X_i. It is important to note that the partial derivatives are typically defined as the sensitivity coefficients.

References

[1] Wangnick K. IDA Worldwide desalting plants. Wangnick Consulting; 2004. 18.
[2] Al-Mutaz IS, Al-Namlah AM. Characteristics of dual purpose MSF desalination plants. Desalination 2004;166:287–94.
[3] Hamed OA, Al-Washmi HA, Al-Otaibi HA. Thermo economic analysis of a power/water cogeneration plant. Energy 2006;31(14):2699–709.
[4] IAEA-TECDOC-942. Thermodynamic and economic evaluation of co-production plants for electricity and potable water. P. Vienna, 1997.
[5] Helal AM. Once-through and brine recirculation MSF designs – a comparative study. Desalination 2005;171(1):33–60.
[6] ElMoudir W, ElBousiffi M, Al-Hengari S. Process modelling in desalination plant operations. Desalination 2008;222(1–3):431–40.
[7] El-Dessouky H, Shaban HI, Al-Ramadan H. Steady-state analysis of multi-stage flash desalination process. Desalination 1995;103(3):271–87.

[8] Hamed OA, Al-Sofi MAK, Iman M, Mustafa GM, Ba MArdouf K, Al-Washmi H. Thermal performance of multi-stage flash distillation plants in Saudi Arabia. Energy Convers Manage 2000;128:281–92.
[9] Kahraman N, Cengel Y. Exergy analysis of a MSF distillation plant. Energy Convers Manage 2005;46:2625–36.
[10] Shivayyanamath S, Tewari PK. Simulation of start-up characteristics of multi-stage flash desalination plants. Desalination 2003;155(3):277–86.
[11] Wangnick K. How incorrectly determined physical and constructional properties in the seawater and brine regimes influence the design and size of an MSF desalination plant – stimulus for further thoughts. In: Proceedings of the IDA, world congress on desalination and water science, Abu Dhabi, vol. 2; 1995. pp. 201–18.
[12] El-Dessouky HT, Ettouney HM. Fundamentals of salt water desalination. Elsevier; 2002.
[13] Serth RW. Process heat transfer: principles and applications; 2007.
[14] Engineering Equation Solver Software. <http://www.fchart.com/>.
[15] Fofonoff P, Millard MA. Algorithms for computation of fundamental properties of seawater. UNESCO Tech.; 1983.
[16] Millero FJ, Chen CT, Bradshaw A, Schleicher K. A new high-pressure equation of state for seawater. Deep-Sea Res 1980;27A:255–64.
[17] Phillip MP, Pender L. A library of MATLAB computational routines for the properties of seawater. Version 3.2 2006, CSIRO.
[18] Lior N. Formulas for calculating the approach to equilibrium in open channel flash evaporators for saline water. Desalination 1986;60:223–49.
[19] Bromley LA, Read SM. Multiple effect flash (MEF) evaporator. Desalination 1970;70:343–91.
[20] Takada M, Drake JC. Application of improved high performance evaporator. Desalination 1983;45:3–12.
[21] Kim JH, Simon TW. Journal of heat transfer policy on reporting uncertainties in experimental measurements and results. J Heat Transfer 1993;115(1):5–6.